

Neural signatures of sleep in zebrafish

Louis C. Leung¹, Gordon X. Wang¹, Romain Madelaine¹, Gemini Skariah¹, Koichi Kawakami², Karl Deisseroth^{3,4,5}, Alexander E. Urban⁶ & Philippe Mourrain^{1,7*}

Slow-wave sleep and rapid eye movement (or paradoxical) sleep have been found in mammals, birds and lizards, but it is unclear whether these neuronal signatures are found in non-amniotic vertebrates. Here we develop non-invasive fluorescence-based polysomnography for zebrafish, and show—using unbiased, brain-wide activity recording coupled with assessment of eye movement, muscle dynamics and heart rate—that there are at least two major sleep signatures in zebrafish. These signatures, which we term slow bursting sleep and propagating wave sleep, share commonalities with those of slow-wave sleep and paradoxical or rapid eye movement sleep, respectively. Further, we find that melanin-concentrating hormone signalling (which is involved in mammalian sleep) also regulates propagating wave sleep signatures and the overall amount of sleep in zebrafish, probably via activation of ependymal cells. These observations suggest that common neural signatures of sleep may have emerged in the vertebrate brain over 450 million years ago.

Sleep has been described in all branches of the animal kingdom using behavioural criteria^{1–3}. This sleep definition has been further expanded to include the main electrophysiological hallmarks of human sleep such as slow-wave sleep (SWS) and paradoxical or rapid eye movement (REM) sleep (abbreviated to PS/REM when referred to collectively), which so far have only been reported in mammals, birds and reptiles^{1,2,4}. It is unclear whether these phenomena exist in non-amniotic vertebrates such as fishes and amphibians, which leaves open the question of whether these states are specific to recent evolution of the neocortex or whether they emerged along with the vertebrate brain over 450 million years ago² (Extended Data Fig. 1a).

In the diurnal vertebrate zebrafish, a bona fide sleep state has been well-established through behavioural criteria; both adult and larval zebrafish exhibit circadian-regulated periods of reversible immobility associated with an increased arousal threshold^{5–7}, as well as sleep rebound in response to sleep deprivation^{6–9}. However, it is difficult to find neuronal sleep signatures in a fish brain because of the absence of a conventional neocortex, at which electroencephalograms (EEG) are typically recorded. Nevertheless, teleost fish possess the dorsal pallium (considered to be a homologue of the neocortex¹⁰), which suggests that sleep signatures might be found by examining this region. Crucially, the major sleep circuits and neuromodulators that are implicated in the regulation of the sleep–wake cycle (such as hypothalamic histamine, hypocretin and melanin-concentrating hormone (MCH), and pontine acetylcholine and GABA) are mostly found in the subcortex, and are well-conserved across vertebrate species from human to zebrafish^{6,9,11} (Extended Data Fig. 1a), which raises the question of whether there are conserved subcortical signatures of sleep.

Neuronal activity in slow oscillating sleep

The compact size and linear rostrocaudal organization of the translucent brain of the larval zebrafish presents an opportunity to identify—in an agnostic fashion—the neuronal sleep signatures that could have pre-existed the radiation of amniotes. We therefore first recorded neuronal activity during sleep in the dorsal pallium of one- to two-week-old zebrafish larvae that expressed the calcium indicator GCaMP6F¹² under a panneuronal promoter¹³ (Fig. 1a, b). To promote

sleep under restraint and light-microscopy conditions, larvae underwent sleep deprivation (Extended Data Fig. 1b, Methods). Behavioural sleep was first assessed by actimetry to ensure optimal conditions for sleep consolidation (Extended Data Fig. 1c–e), as previously established^{5,7,9}. After sleep deprivation, larvae were imaged at single-cell resolution for dorsal pallium activity, and compared to non-sleep-deprived sibling controls. We observed that in awake, non-sleep-deprived fish high spontaneous activity in the telencephalon occurred at the anterolateral regions of the dorsal pallium, and was desynchronous (Fig. 1c, e, see Supplementary Information, supplementary video 1). Notably, when asleep, sleep-deprived fish displayed highly synchronous bursts of activity punctuated by periods of silence in the dorsal pallium (Fig. 1d, f, see Supplementary Information, supplementary video 2). Quantification of activity in each pallial hemisphere of sleep-deprived versus non-sleep-deprived brains showed significant shifts in three metrics of activity and synchronicity within and between hemispheres: periodicity (the inter Ca²⁺ transient interval (ITI)), amplitude and coherence index (coincident firing of >50% of a population per epoch (Methods, Supplementary Fig. 1)). During sleep, the average interval of firing activity was longer (sleep-deprived ITI of 12.26 ± 2.91 s versus non-sleep-deprived ITI of 3.84 ± 0.14 s) (Extended Data Fig. 1f), and—in sleep-deprived fish—the average burst intensity of Ca²⁺ transients was higher in sleep than those observed during wake (25.75 ± 0.29% increase in spike fluorescence) (Fig. 1d, f). The coherence index, which measures inter-neuronal synchronicity, was significantly higher for sleep-deprived brains compared to non-sleep-deprived (18.84% versus 6.38%, respectively) (Fig. 1d, f). Further, the probability of observing the signature of what we here term slow bursting sleep (SBS) (synchronous ITI band of 5–30 s) increased with the duration of sleep deprivation (non-sleep-deprived 0%, 1-d sleep deprivation 25%, 2-d sleep deprivation 57% and 3-d sleep-deprivation 71%) (Extended Data Fig. 1g), which suggests that the occurrence of SBS activity in zebrafish is proportional to sleep pressure (sleep homeostasis).

Pallial sleep signatures with hypnotics

We next investigated whether sleep-related neuronal activities, such as the SBS signature, could be induced with hypnotic compounds.

¹Center for Sleep Sciences and Medicine, Department of Psychiatry and Behavioral Sciences, Stanford University, Stanford, CA, USA. ²Division of Molecular and Developmental Biology, National Institute of Genetics and Department of Genetics, Sokenkai, Mishima, Japan. ³Howard Hughes Medical Institute, Stanford, CA, USA. ⁴Department of Bioengineering, Stanford University, Stanford, CA, USA. ⁵Department of Psychiatry and Behavioral Sciences, Stanford University, Stanford, CA, USA. ⁶Center for Genomics and Personalized Medicine, Department of Psychiatry and Behavioral Sciences, Stanford University, Stanford, CA, USA. ⁷INSERM 1024, Ecole Normale Supérieure, Paris, France. *e-mail: mourrain@stanford.edu

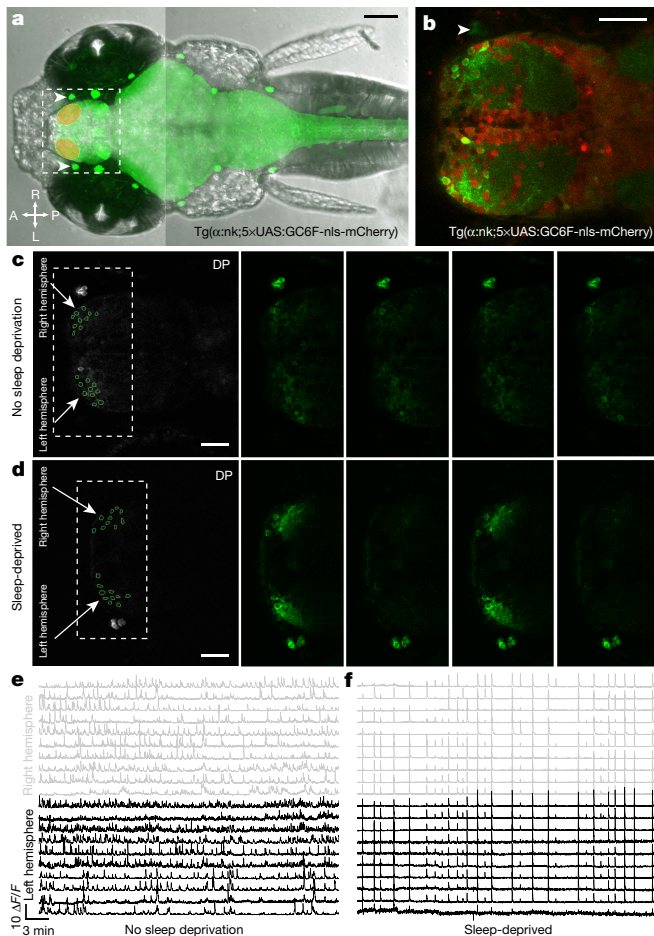


Fig. 1 | Sleep deprivation produces slow bursting activity in the zebrafish dorsal pallium. **a**, Dorsal view of a brain from Tg(*a:nk;5×UAS:GCaMP6F-p2a-nls-mCherry*) (see Methods for details of zebrafish lines) zebrafish at seven days post-fertilization (only GCaMP is shown), superimposed on its body plan (transmitted light). Orange ovals depict anterolateral dorsal pallium, at which high spontaneous awake activity occurs. Scale bar, 100 μm . A, anterior; L, left; R, right; P, posterior. **b**, Single *z*-slice image of the telencephalic region (GCaMP (green) and nuclear-localized mCherry (red)) from dashed box in **a**, at the level of the neuromast fiduciary marker (white arrowhead). Scale bar, 50 μm . **c, d**, Left, representative images showing 20 masks on non-sleep-deprived (**c**) or sleep-deprived (**d**) brains. Right, magnified clips of Ca^{2+} imaging in the dorsal pallium (DP) from the region in dashed box in the leftmost panel. Scale bars, 50 μm . **e, f**, Time-aligned $\Delta F/F$ traces of the 20 neurons from non-sleep-deprived fish (**e**) marked in **c** and sleep-deprived fish (**f**) marked in **d**. Desynchronous versus synchronous indices, ITI: 3.84 ± 0.14 s versus 12.26 ± 2.91 s; $P = 0.00018$, Wilcoxon rank-sum test $n = 10$ fish per condition; coherence index, 6.32% ($n = 40,175$ spikes) versus 18.84% ($n = 41,161$ spikes); $P < 0.05$, χ^2 test.

Stimulation of non-sleep-deprived fish with hypnotics at doses that induce behavioural sleep states (Supplementary Table 1) revealed three categories of neuronal signature in the dorsal pallium (Fig. 2b, c, Extended Data Fig. 2): SBS, broad silencing and waveforms that travel in a caudal-to-rostral direction (see Supplementary Information for description of dimensionality reduction in Fig. 2). Unlike carrier controls (Fig. 2a), intra- and inter-hemispheric SBS were induced by the histamine receptor (H1R) antagonists mepyramine (Fig. 2b, see Supplementary Information, supplementary video 3) and promethazine (Extended Data Fig. 2a). We found increased slow synchronous activity upon treatment with these compounds, as shown by changes in the ITI (4.42 ± 0.38 s versus 16.55 ± 6.79 s), amplitude (25.37% increase) and coherence index (6.06% versus 31.18%) between baseline

and mepyramine dynamics. Similar to sleep deprivation, H1R antagonism in zebrafish increases neuronal network synchronicity, resulting in slower-frequency, higher-amplitude neuronal bursts in the dorsal pallium of sleeping fish; together, these observations reflect a state that shares commonalities with mammalian SWS. Indeed, EEG slow waves reflect the oscillation of synchronized on-off activity in cortical neurons¹⁴. Similar to the role of slow-wave activity as the primary indicator of the length of prior wakefulness or sleep pressure^{15,16}, we found that increases in SBS were proportional to the duration of sleep deprivation. Indeed, in rodents and cats, H1R antagonism specifically increases and consolidates SWS at the expense of REM sleep^{17–19}. However, a notable difference between SBS dynamics and SWS is the relatively slower speed of the former (see Supplementary Information for discussion of the infra-slow band (<0.1 Hz)). Our data suggest that synchronous oscillatory neuronal states during sleep may have arisen earlier than previously expected in the evolution of the vertebrate nervous system.

Unlike SBS, the hypnotic GABA_A-receptor agonist gaboxadol and the anaesthetic MS222 induced sustained silencing in overall activity in the dorsal pallium (Extended Data Fig. 2b, c, see Supplementary Information, supplementary videos 4, 5). It has previously been reported in mice that a broad reduction in overall cortical activity occurs during sleep²⁰, which suggests that this reduction might be a feature of sleep and would be consistent with the hypnotic effect of gaboxadol in flies²¹. However, it is doubtful that such total, unbiased shutdown of firing represents a bona fide sleep state; the similarity between the states induced by gaboxadol and the MS222 anaesthetic therefore led us to reject this compound from further study.

The final category of sleep signature is characterized by travelling waves of neuronal activity that spread anteriorly across the telencephalon. This specific signature was induced by three compounds: the non-benzodiazepine imidazopyridine hypnotic zolpidem²² (Extended Data Fig. 2d, see Supplementary Information, supplementary video 6), the cholinomimetic carbachol (Fig. 2c, see Supplementary Information, supplementary video 7) and eserine²³, an acetylcholine esterase inhibitor (Extended Data Fig. 2e). We observed a sequence of activations that started with a noticeable relaxation of the telencephalon (seen by tissue distention; see Supplementary Information, supplementary video 7), followed by a stereotyped caudal-to-rostral midline activation, and then by a high-amplitude wave (with a mean duration of about 2.5 min) that swept through the telencephalon (Fig. 2c). After this transient wave, there is a return to desynchronized activity in the dorsal pallium. Together, we find that—at the dorsal pallium—at least two neuronal sleep signatures are revealed at single-cell resolution: SBS and travelling waves.

Fluorescence-based polysomnography for SBS

As sleep is a body-wide phenomenon that cannot be defined solely by a telencephalic neuronal signature, we sought to incorporate a measure of the physiological parameters used to define sleep through polysomnography (PSG). We developed an imaging platform that combined a custom light-sheet microscope—which enables high-speed, wide-field and pixel-synchronous acquisition across the animal (Fig. 3a)—with a transgenic zebrafish line (which we named ‘zPSG’) that expresses GCaMP7a in the brain and trunk muscles and GFP in the heart (Fig. 3b, Methods) to perform fluorescence-based (f)PSG. fPSG recapitulates PSG in fish (Fig. 3c) through proxies for brain activity (an fEEG), muscle activity (a fluorescence-based electromyogram (fEMG)), heart rate (a fluorescence-based electrocardiogram (fECG)) and eye movement (a fluorescence-based electrooculogram (fEOG)).

Consistent with our telencephalic imaging, both sleep deprivation and treatment with antihistamines revealed intra- and inter-hemispheric synchronicity in the dorsal pallium during fPSG, along with broadly reduced ‘subcortical’ brain activity (Extended Data Fig. 3a–e, see Supplementary Information, supplementary video 13). Compared to the wake state, an associated decrease in Ca^{2+} transients in trunk muscle cells was observed during SBS, which is consistent with reduced actimetry during sleep (fEMG in Fig. 3d). Analysis of eye

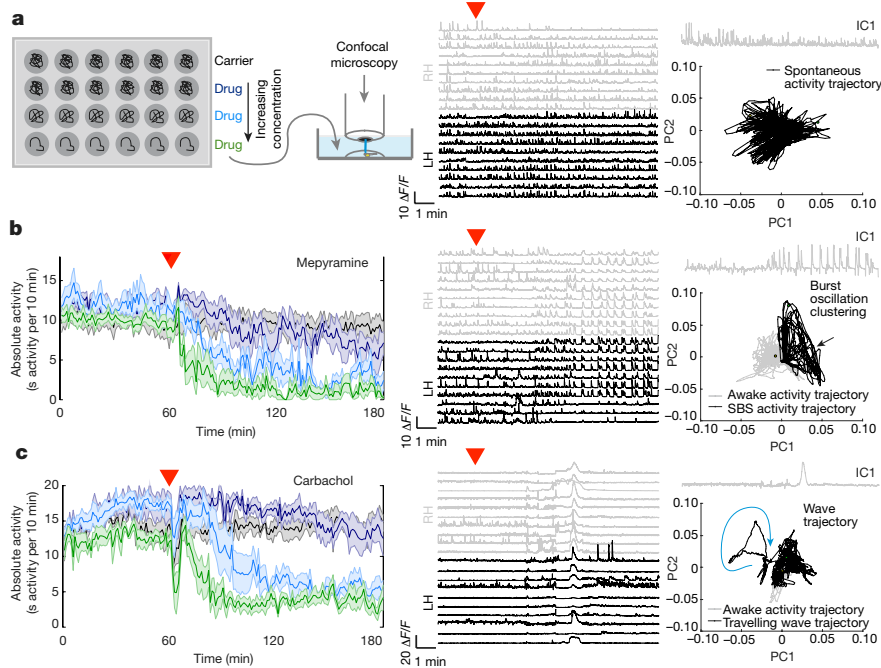


Fig. 2 | Hypnotics induce heterogeneous effects on telencephalic activity. **a**, Left, schematic of experimental pipeline. Compounds are first validated as hypnotic by screening freely behaving fish, before being applied to agar-restrained fish for Ca^{2+} imaging. Middle, time-aligned $\Delta F/F$ traces of 20 randomly selected dorsal pallium neurons from a carrier-stimulated fish (red triangle indicates addition after 10 min). Right, neural signature across all time points represented by the first independent component (IC) (top) or replotted following principal components analysis (PCA) (bottom). LH, left hemisphere; RH, right hemisphere. **b**, **c**, Left, three-hour actimetry recordings, in which a range of drug dosages were added after one hour (red triangle). Activity traces are expressed as the number of seconds active per ten-minute time bin,

movement also showed a notable absence of saccades (fEOG in Fig. 3d). The heart rate decreased on average twofold, from about 200 beats per minute during wakefulness to about 110 beats per minute during sleep rebound or about 110 beats per minute upon treatment with mepyramine (fECG in Fig. 3d), and maintained a tight distribution of interbeat intervals (about 500–600 ms) (fECG in Fig. 3d, Extended Data Fig. 4).

To confirm that SBS also occurs during the normal circadian night, we implemented a wake-maintenance method to gently consolidate wake (and thus subsequent sleep) during daylight hours, before performing night-phase fPSG (Methods). Similar to sleep rebound and treatment with antihistamine, we observed SBS (as defined by fPSG) during the normal circadian night (Extended Data Figs. 9, 10). Finally, we found that habituation to agarose restraint of untreated larvae allowed spontaneous expression of SBS signatures during normal circadian night (Extended Data Fig. 11, Methods, see Supplementary Information, supplementary video 17). Together, fPSG experiments demonstrated that during sleep induced by hypnotics, sleep rebound, sleep after wake maintenance and spontaneous sleep, SBS is tightly associated with synchronous dorsal pallium activity and with reductions in muscle, eye and cardiorespiratory activity. These features confirm behavioural observations of sleep states in fish, and share polysomnographic commonalities with non-REM SWS in mammals, birds and reptiles.

fPSG for propagating wave sleep

Our data showed travelling waves that arrived from beyond the telencephalon, which prompted us to use fPSG to fully capture the generation of this sleep signature. Expanding our analysis to the whole-brain scale allowed us to uncover a rich fluid sequence that starts with a bilateral anteroposterior wave of muscular activation, midline and

and plotted as trial-averaged mean (solid line) \pm s.e.m. (shaded) per dose of mepyramine (**b**, $n = 24$ fish), and carbachol (**c**, $n = 24$ fish) from low to high (black < purple < blue < green; see Supplementary Table 1 for concentrations), showing induction of dose-responsive behavioural sleep. Middle and right plots show representative time-aligned $\Delta F/F$ traces, independent component analysis and PCA (grey and black lines depict wake and sleep dynamics, respectively) for respective drugs. Wake versus mepyramine SBS synchronicity indices: ITI, 4.42 ± 0.38 s versus 16.55 ± 6.79 s, $P = 0.041$, Wilcoxon rank-sum test, $n = 6$ fish and coherence index 6.06% ($n = 5,177$ spikes) versus 31.18% ($n = 7,215$ spikes), $P < 0.00001$, χ^2 test. See Supplementary Information for reproducibility information.

ventricular zone activation, followed by a travelling wave of neuronal activation that propagates rostrally from the pons to the telencephalon, as seen on treatment with carbachol (fEEG in Fig. 3e, Extended Data Fig. 3h; detailed staging is shown in Supplementary Information, supplementary videos 8, 9, 19), eserine (Extended Data Fig. 5b, see Supplementary Information, supplementary video 10) or zolpidem (Extended Data Fig. 5e, see Supplementary Information, supplementary video 11). Inductions of these activities with either carbachol or eserine were blocked by pre-incubation with methoctramine, an inhibitor of muscarinic acetylcholine receptors (M2 and M4) (Extended Data Fig. 5c, d), which confirmed the specific involvement of cholinergic neurotransmission. We refer to the brain wave dynamic that is common to cholinergic and GABAergic induction as the ponto-midbrain-telencephalic (PMT) wave.

While the fPSG initially recorded the normal awake profile that features frequent eye saccades, active muscle tone and a heart rate of about 200 beats per minute (with a regular interbeat interval of about 300 ms) (Fig. 3e, see Supplementary Information, supplementary videos 9, 16), the PMT wave marked the onset of a sleep state that we term propagating wave sleep (PWS) (Fig. 3e, Extended Data Fig. 3f–h), which has features that are consistent with previously recorded cholinergic and GABAergic-induced behavioural sleep. First, muscle activity showed a rapid and total loss of muscle tone, which persisted (fEMG in Fig. 3e). Second, spontaneous eye movements gave way to a slow roll (relaxation; black box in the fEOG panel of Fig. 3e) before stopping entirely. Third, the heart rate not only dropped to about 90 beats per minute but also showed increased variance in the distribution of interbeat intervals (700–1,100 ms, coefficient of variation 0.13 versus 0.64) (fECG in Fig. 3e, Extended Data Fig. 4a, d). This PWS state is distinct from SBS, in which muscle tone decreased but was not absent and heart

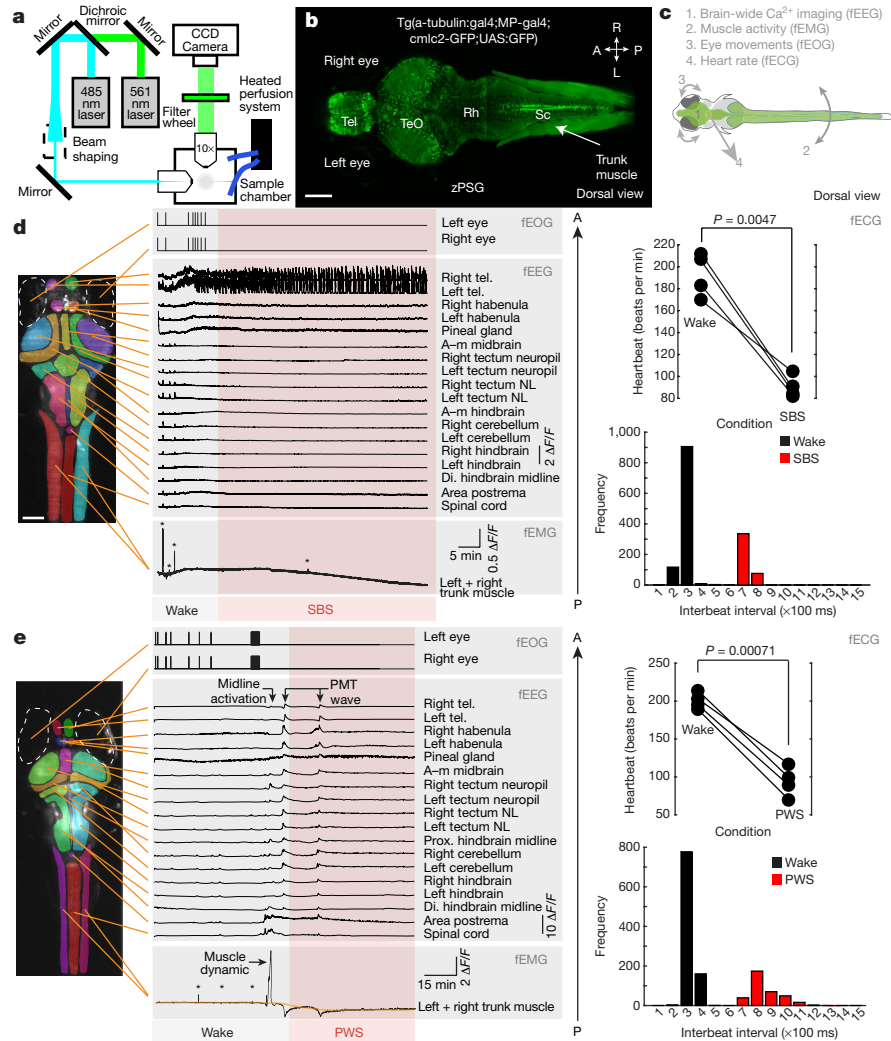


Fig. 3 | Fluorescence-based polysomnography reveals SBS and PWS in zebrafish. **a**, Schematic diagram of the light-sheet microscope platform (based on the openSPIM design; see ‘fPSG’ in ‘Sample preparation and Ca²⁺ imaging’ in Methods) used to take time-lapse recordings of synchronous *x–y* frames as single slices or volumes customized with temperature control and drug perfusion apparatus. **b**, Single *z*-plane (dorsal view) of a zPSG transgenic fish at seven days post-fertilization, co-expressing a trunk muscle *gal4* and pan-neuronal *gal4* used to drive expression of *UAS:GCaMP7a*. Broad brain regions are indicated as telencephalon (Tel), optic tectum (TeO), rhombencephalon (Rh) and spinal cord (Sc). Scale bar, 100 μ m. **c**, Depiction of parameters that can be measured, based on fluorescent markers of zPSG fish that form

an fPSG. **d, e**, Left, broad fPSG region-of-interest masks on a maximum projection image to measure GCaMP activity before, during and after initiation of SBS (**d**) or PWS (**e**). Middle, Brain and muscle activity traces ($\Delta F/F$) from broad regions defined by masks (middle panels show fEEG and bottom panels show fEMG), with integration of activity across 1 s (**d**) or 2.5 s (**e**) bins. Asterisks denote muscle contractions. Time trace of eye movements (fEOG) is shown in the top panels. Right, heart rate (fECG), measured before and after recording of SBS (**d**) or PMT wave (**e**) (top), and distribution of interbeat intervals (bottom). **P* < 0.05. Two-sided paired *t*-test, *n* = 4 fish per condition. A–m, anteromedial; di., distal; NL, neuronal layer; prox., proximal.

beat was slow but regular (coefficient of variation 0.18 versus 0.13) (Extended Data Fig. 4). Unlike in SBS (in which dorsal pallium neurons oscillate synchronously between on and off activity), desynchronous activity close to ITIs and coherence indices observed during the wake state is resumed after the PMT wave (pre-PMT wave versus post-PMT wave ITI 2.88 ± 2.14 s versus 2.96 ± 1.35 s; coherence index, 1.32% versus 1.08%) (Extended Data Fig. 3f, g).

As with SBS, we further sought to examine the presence of PMT waves and subsequent dynamics during daytime sleep rebound after sleep deprivation, during night-phase sleep after wake maintenance and after habituation of untreated larva. Confirming pharmacologically induced PMT signatures, we observed that, after sleep deprivation, there were rare instances of PWS dynamics that included extended periods of midline ventricular activation before the onset of PMT waves (see Supplementary Information, supplementary video 12). Finally, in normal night-phase sleep, we found spontaneous PMT waves that

were associated with muscle atonia and wake-like active dorsal pallium (Extended Data Figs. 10, 11, Supplementary Fig. 2 and Supplementary Information, supplementary video 18).

PWS is reminiscent of PS/REM, with which it shares at least six commonalities—including pontine waveforms (PMT versus ponto-geniculo-occipital waves^{24,25}), wake-like activity in dorsal pallium (equivalent to paradoxical activity in PS/REM), a total loss of muscle tone, increased variability in heart rate, induction by cholinergic or GABAergic agonists^{23,26}, and blockade by M2 and M4 antagonists^{27,28}. One notable difference between PWS and REM is the absence of the hallmark rapid eye movements of the eponymous mammalian sleep state. This is consistent with the absence of rapid eye movements during adult zebrafish sleep, despite the fact that other physiological features of PS/REM (such as slow and irregular breathing) remain present²⁹. Future studies in fishes and other non-mammalian vertebrates will uncover whether PWS is analogous to PS/REM.

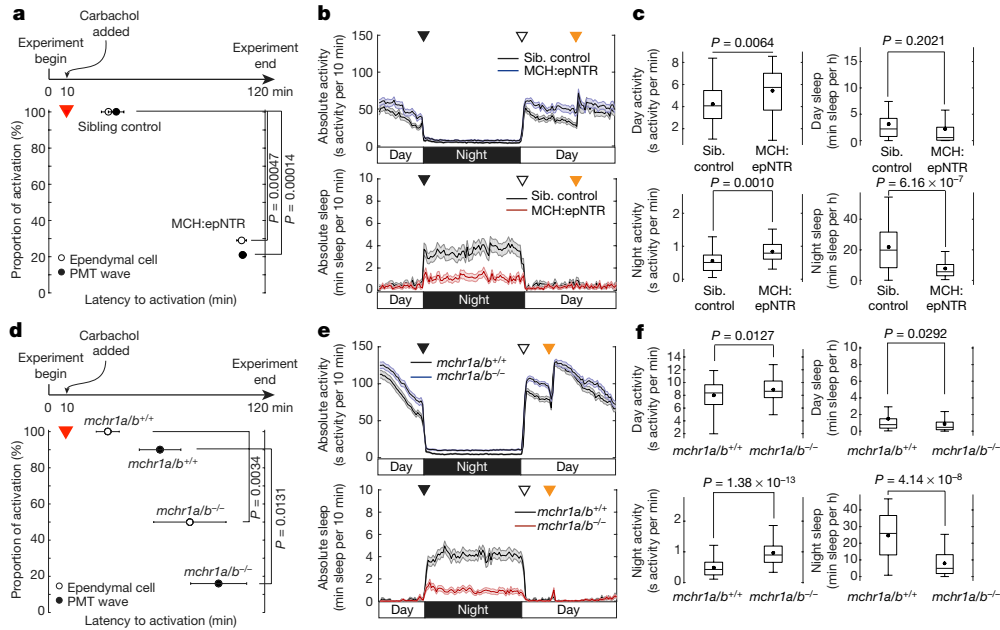


Fig. 4 | MCH signalling is required for sleep and generation of PWS dynamics. a–f, MCH2 neuron-ablated (a–c) and MCHR mutant (d–f) fish display increased activity, decreased sleep and disrupted onset of ependymal cell and PMT-wave dynamics. a, d, Top, timeline of a two-hour Ca^{2+} imaging experiment with addition of the PWS inducer (red triangle). Bottom, proportion of sibling (sib.)-treated control ($n = 10$ fish) versus MCH2-ablated ($n = 14$ fish) groups (a) or $mchr1a^{+/+}mchr1b^{+/+}$ ($mchr1a/b^{+/+}$) controls ($n = 10$ fish) versus $mchr1a^{-/-}mchr1b^{-/-}$ ($mchr1a/b^{-/-}$) double mutants ($n = 6$ fish) (d) with ependymal (open circle) and/or PMT-wave (filled circle) activation within the imaging session, plotted against the mean latency to activation (min) \pm s.e.m. * $P < 0.05$ χ^2 test. b, e, Top, actimetry of sibling-treated control ($n = 42$) versus MCH2-

neuron-ablated ($n = 44$) fish (b) or $mchr1a^{+/+}mchr1b^{+/+}$ ($n = 67$) versus $mchr1a^{-/-}mchr1b^{-/-}$ double mutant ($n = 72$) fish (e) in 10-min bins over a 24-h period, showing mean seconds of activity per bin (bold) \pm s.e.m. (shaded). Bottom, sleep depicted as minutes per 10-min bin \pm s.e.m. (shaded). Black or white triangles indicate day-to-night or night-to-day transitions, respectively, and orange triangles show time of feeding. c, f, Box plots showing spread of total activities and sleep between sibling-treated control versus MCH2-neuron-ablated (c) or $mchr1a^{+/+}mchr1b^{+/+}$ versus $mchr1a^{-/-}mchr1b^{-/-}$ double (f) groups separated out by day and night. Blue lines and black circles denote the median and mean, respectively. Two-sided Student's t -test.

Ependymal cells as precursors to sleep onset

Our unbiased, brain-wide activity screen provided an opportunity to find novel cell types that are potentially involved in sleep regulation. Notably, a motif that appeared robustly at the onset of the PWS activome was the midline-cell activation that appeared to span the anteroposterior axis of the brain (panel h2 in Extended Data Fig. 3). We serendipitously identified a zebrafish line that expressed mCherry in cells that matched the characteristic ventricular location, triangular cell morphology and long thin processes of the activated cells (Extended Data Fig. 6b, c). By crossing this line with our zPSG line, we confirmed that a large subset of mCherry-positive cells were the same periventricular cell types that were activated before the PMT wave (Extended Data Fig. 6d–f) and subsequently inactivated as the wave continued through the brain (Extended Data Fig. 6f, g, Supplementary Information, supplementary video 14). On the basis of their positioning and morphology, and the fact that they were α -tubulin-positive and largely glial fibrillary acidic protein (GFAP)-negative at this developmental stage³⁰ (Extended Data Fig. 6b, c), we consider these cells to be specialized ependymal cells or perhaps tanycytes, which have known functions in controlling the flow of cerebrospinal fluid^{31–33}. The attempted physical removal of ependymal cells to examine their roles proved lethal, probably owing to the critical roles of these cells in maintaining periventricular tissue integrity (Extended Data Fig. 7; see Supplementary Information for detailed description). As sleep regulators such as hypocretin (also known as orexin), MCH, histamine and other neurotransmitters can signal through the cerebrospinal fluid (potentially via ependymal cells), we sought other methods to probe the functional role of ependymal cells in PWS dynamics in zebrafish.

Ependymal cells, MCH, pigments and sleep

A conserved property of ependymal cells is their activation by MCH, which is a well-known modulator of sleep³⁴ and skin pigmentation³⁵. Ciliated ependymal cells express MCH³⁶ and MCHR1³¹, and *ex vivo* experiments have shown the former can stimulate increased Ca^{2+} transients that upregulate ciliary beat frequency^{31,37}, which led us to ask whether MCH could directly activate zebrafish ependymal cells. To examine this, we injected MCH into the intracerebroventricular cavity of zPSG fish (Extended Data Fig. 7h). Significant increases in GCaMP fluorescence in periventricular cells in response to MCH, compared to mock- or carrier-injected fish (-0.98% versus $+53.74\%$) (Extended Data Fig. 6h–m), provides functional evidence for their identity as ependymal cells and their potential involvement in the MCH-dependent regulation of sleep. Consistent with the association between MCH and its pigmentation functions in fish, we uncovered a notable coupling of epidermal melanin spreading and contraction to ependymal cell activation and PMT waves (Extended Data Fig. 6, Supplementary Information for detailed description, Supplementary Information, supplementary video 15). This finding not only points to MCH as a key mediator in coregulating pigmentation and sleep dynamics in zebrafish, but also has implications for the many vertebrate species (including fishes, amphibians and reptiles) that adapt their coloration during sleep as cryptic or aposematic strategies to avoid predation.

In mammals, MCH neurons fire maximally during REM sleep³⁸; optogenetic activation, as well as intracerebroventricular injection with MCH peptide, can promote REM^{34,39}. MCH2 has previously been identified as the true homologue in fishes of mammalian MCH, as well as its receptors¹¹. We therefore used three loss-of-function strategies to examine the role of MCH signalling in both regulating PWS signatures

(ependymal cell activation and PMT waves) and the overall amount of behavioural sleep.

First, to test whether the removal of MCH2 neurons disrupted sleep brain signatures and behaviour, a fish line that expresses enhanced nitroreductase under the control of the MCH2 promoter was generated and crossed into the zPSG line (Extended Data Fig. 8a, b). Chemogenetic ablation was induced by incubation with metronidazole. When imaged in a two-hour incubation of carbachol, MCH2-neuron-ablated fish produced far fewer ependymal cell activations (100% versus 29%) or PMT waves (100% versus 21%) than sibling transgene-negative controls treated with metronidazole—and those activations that did occur were significantly delayed (Fig. 4a). In parallel, actimetry over an entire sleep–wake cycle of free-swimming MCH2-neuron-ablated transgenic fish revealed a twofold decrease in the amount of sleep during the night, as compared to treated sibling controls (Fig. 4b, c, Supplementary Table 2).

Second, we used the MCHR1 inhibitor H6408, which has previously been shown to prevent the MCH modulation of ciliary beat frequency in ependymal cells³⁷. Pre-incubation of H6408 significantly affected the ability of carbachol to activate ependymal cells (100% versus 42%) and PMT waves (88.5% versus 42%) in zPSG fish (Extended Data Fig. 8k). In actimetry experiments, there was an initial marked increase in basal activity after a two-hour H6408 incubation, although this transient effect did not significantly affect long-term sleep patterning at these concentrations (Extended Data Fig. 8l, m, Supplementary Table 2).

Finally, for the constitutive disruption of MCHR signalling in zPSG fish, we generated double mutants against both subtypes of MCHR1 (MCHR1a and MCHR1b) using CRISPR–Cas9 and TILLING approaches, respectively (Fig. 4d–f). These MCHR1a MCHR1b double mutants exhibit significant disruption of ependymal cell activation (100% versus 50%) and induction of PMT waves (90% versus 16%), with a marked delay relative to non-mutants (Fig. 4d). Consistent with the disruption in their sleep neuronal signatures, the double-mutant (*mchr1a*^{-/-}*mchr1b*^{-/-}) zebrafish displayed increases in day and night activity with a significant reduction in the amount of sleep at night compared to non-mutants (*mchr1a*^{+/+}*mchr1b*^{+/+}) (Fig. 4e, f, Supplementary Table 2). These results show that MCH signalling has an important role in activating the PWS signature, and in regulating the amount of sleep, in zebrafish.

Discussion

Over a century ago, behavioural criteria were established that enabled the first scientific description of the sleep state in fishes³. Here we identify the first neuronal sleep signatures in teleost fishes: slow synchronous ON–OFF oscillations in the dorsal pallium (the SBS state) and a sleep state initiated with propagating waves (the PWS state), both of which occur in an overall background of reduced brain activity (see Supplementary Information for discussion of silencing as a signature). SBS and PWS dynamics share many commonalities with those of SWS and PS/REM, respectively, which suggests that sleep-related neuronal signatures coupled with characteristic muscular signatures (in heart, eye and voluntary muscle) may have emerged much earlier than the radiation of amniotes (about 450 million years ago), and that they probably mark ancestral sleep functions that are essential across vertebrates.

Using cellular-resolution polysomnography in zebrafish, we have identified the very first neural cells that are activated before PWS, and often before SBS: the periventricular ependymal cells. Ependymal cells express MCHR³⁷ and, as ciliated cells, participate in the flow of sleep-related neurotransmitters throughout the ventricular system of the brain (see Supplementary Information for discussion of potential roles of ependymal cells in sleep). We found that fish ependymal cells are activated by MCH; this neuropeptide is implicated in mammalian REM, but its role in sleep in fishes has been under debate since its discovery in salmon in 1983⁴⁰. We show that disruption of the MCH signal perturbs PWS and greatly reduces sleep quantity, which suggests that it has a sleep-promoting role in fishes that is similar to its role in

mammals (see Supplementary Information for discussion of the sleep role of MCH in fishes).

fPSG enables the non-invasive holistic capture of the choreography of physiological responses that are required for sleep–wake regulation. The agnostic identification of new sleep substrates paves the way for the investigation of cellular and molecular mechanisms that could potentially generate therapeutic targets. The power of fPSG could also be harnessed to profile hypnotics on the basis of not only the central nervous system activitome but also their cellular effect on organ systems that are optically accessible in the zebrafish, a platform that has the potential to be extended to model sleep disorders or other complex psychiatric behaviours.

Online content

Any methods, additional references, Nature Research reporting summaries, source data, statements of data availability and associated accession codes are available at <https://doi.org/10.1038/s41586-019-1336-7>.

Received: 13 October 2017; Accepted: 30 May 2019;

Published online 10 July 2019.

- Campbell, S. S. & Tobler, I. Animal sleep: a review of sleep duration across phylogeny. *Neurosci. Biobehav. Rev.* **8**, 269–300 (1984).
- Leung, L. C. & Mourrain, P. Sleep: short sleepers should keep count of their hypocretin neurons. *Curr. Biol.* **28**, R558–R560 (2018).
- Pieron, H. *Le Probleme Physiologique su Sommeil* (Masson, 1913).
- Shein-Idelson, M., Ondracek, J. M., Liaw, H. P., Reiter, S. & Laurent, G. Slow waves, sharp waves, ripples, and REM in sleeping dragons. *Science* **352**, 590–595 (2016).
- Prober, D. A. et al. Hypocretin/orexin overexpression induces an insomnia-like phenotype in zebrafish. *J. Neurosci.* **26**, 13400–13410 (2006).
- Yokogawa, T. et al. Characterization of sleep in zebrafish and insomnia in hypocretin receptor mutants. *PLoS Biol.* **5**, e277 (2007).
- Zhdanova, I. V. Sleep in zebrafish. *Zebrafish* **3**, 215–226 (2006).
- Aho, V. et al. Homeostatic response to sleep/rest deprivation by constant water flow in larval zebrafish in both dark and light conditions. *J. Sleep Res.* **26**, 394–400 (2017).
- Appelbaum, L. et al. Sleep–wake regulation and hypocretin–melatonin interaction in zebrafish. *Proc. Natl Acad. Sci. USA* **106**, 21942–21947 (2009).
- Mueller, T., Dong, Z., Berberoglu, M. A. & Guo, S. The dorsal pallium in zebrafish, *Danio rerio* (Cyprinidae, Teleostei). *Brain Res.* **1381**, 95–105 (2011).
- Berman, J. R., Skariah, G., Maro, G. S., Mignot, E. & Mourrain, P. Characterization of two melanin-concentrating hormone genes in zebrafish reveals evolutionary and physiological links with the mammalian MCH system. *J. Comp. Neurol.* **517**, 695–710 (2009).
- Chen, T. W. et al. Ultrasensitive fluorescent proteins for imaging neuronal activity. *Nature* **499**, 295–300 (2013).
- Madelaine, R. et al. MicroRNA-9 couples brain neurogenesis and angiogenesis. *Cell Reports* **20**, 1533–1542 (2017).
- Chauvette, S., Crochet, S., Volgushev, M. & Timofeev, I. Properties of slow oscillation during slow-wave sleep and anesthesia in cats. *J. Neurosci.* **31**, 14998–15008 (2011).
- Borbély, A. A. A two process model of sleep regulation. *Hum. Neurobiol.* **1**, 195–204 (1982).
- Borbély, A. A., Daan, S., Wirz-Justice, A. & Deboer, T. The two-process model of sleep regulation: a reappraisal. *J. Sleep Res.* **25**, 131–143 (2016).
- Ikedo-Sagara, M. et al. Induction of prolonged, continuous slow-wave sleep by blocking cerebral H₁ histamine receptors in rats. *Br. J. Pharmacol.* **165**, 167–182 (2012).
- Marzanatti, M., Monopoli, A., Trampus, M. & Ongini, E. Effects of non-sedating histamine H₁-antagonists on EEG activity and behavior in the cat. *Pharmacol. Biochem. Behav.* **32**, 861–866 (1989).
- Saitou, K., Kaneko, Y., Sugimoto, Y., Chen, Z. & Kamei, C. Slow wave sleep-inducing effects of first generation H₁-antagonists. *Biol. Pharm. Bull.* **22**, 1079–1082 (1999).
- Niethard, N. et al. Sleep-stage-specific regulation of cortical excitation and inhibition. *Curr. Biol.* **26**, 2739–2749 (2016).
- Dissel, S. et al. Sleep restores behavioral plasticity to *Drosophila* mutants. *Curr. Biol.* **25**, 1270–1281 (2015).
- Che Has, A. T. et al. Zolpidem is a potent stoichiometry-selective modulator of $\alpha 1\beta 3$ GABA_A receptors: evidence of a novel benzodiazepine site in the $\alpha 1$ – $\alpha 1$ interface. *Sci. Rep.* **6**, 28674 (2016).
- Sitaram, N., Wyatt, R. J., Dawson, S. & Gillin, J. C. REM sleep induction by physostigmine infusion during sleep. *Science* **191**, 1281–1283 (1976).
- Callaway, C. W., Lydic, R., Baghdoyan, H. A. & Hobson, J. A. Pontogeniculooccipital waves: spontaneous visual system activity during rapid eye movement sleep. *Cell. Mol. Neurobiol.* **7**, 105–149 (1987).
- Datta, S. Cellular basis of pontine ponto-geniculo-occipital wave generation and modulation. *Cell. Mol. Neurobiol.* **17**, 341–365 (1997).
- Baghdoyan, H. A., Lydic, R., Callaway, C. W. & Hobson, J. A. The carbachol-induced enhancement of desynchronized sleep signs is dose dependent and antagonized by centrally administered atropine. *Neuropsychopharmacology* **2**, 67–79 (1989).

27. Coleman, C. G., Lydic, R. & Baghdooyan, H. A. M2 muscarinic receptors in pontine reticular formation of C57BL/6J mouse contribute to rapid eye movement sleep generation. *Neuroscience* **126**, 821–830 (2004).
28. Datta, S., Quattrochi, J. J. & Hobson, J. A. Effect of specific muscarinic M2 receptor antagonist on carbachol induced long-term REM sleep. *Sleep* **16**, 8–14 (1993).
29. Arnason, B. B., Þorsteinsson, H. & Karlsson, K. A. E. Absence of rapid eye movements during sleep in adult zebrafish. *Behav. Brain Res.* **291**, 189–194 (2015).
30. Roessmann, U., Velasco, M. E., Sindely, S. D. & Gambetti, P. Glial fibrillary acidic protein (GFAP) in ependymal cells during development. An immunocytochemical study. *Brain Res.* **200**, 13–21 (1980).
31. Conductier, G. et al. Control of ventricular ciliary beating by the melanin concentrating hormone-expressing neurons of the lateral hypothalamus: a functional imaging survey. *Front. Endocrinol.* **4**, 182 (2013).
32. Dale, N. Purinergic signaling in hypothalamic tanycytes: potential roles in chemosensing. *Semin. Cell Dev. Biol.* **22**, 237–244 (2011).
33. Rizzoti, K. & Lovell-Badge, R. Pivotal role of median eminence tanycytes for hypothalamic function and neurogenesis. *Mol. Cell. Endocrinol.* **445**, 7–13 (2017).
34. Peyron, C., Sapin, E., Leger, L., Luppi, P. H. & Fort, P. Role of the melanin-concentrating hormone neuropeptide in sleep regulation. *Peptides* **30**, 2052–2059 (2009).
35. Logan, D. W., Burn, S. F. & Jackson, I. J. Regulation of pigmentation in zebrafish melanophores. *Pigment Cell Res.* **19**, 206–213 (2006).
36. Torterolo, P., Lagos, P., Sampogna, S. & Chase, M. H. Melanin-concentrating hormone (MCH) immunoreactivity in non-neuronal cells within the raphe nuclei and subventricular region of the brainstem of the cat. *Brain Res.* **1210**, 163–178 (2008).
37. Conductier, G. et al. Melanin-concentrating hormone regulates beat frequency of ependymal cilia and ventricular volume. *Nat. Neurosci.* **16**, 845–847 (2013).
38. Hassani, O. K., Lee, M. G. & Jones, B. E. Melanin-concentrating hormone neurons discharge in a reciprocal manner to orexin neurons across the sleep–wake cycle. *Proc. Natl Acad. Sci. USA* **106**, 2418–2422 (2009).
39. Jego, S. et al. Optogenetic identification of a rapid eye movement sleep modulatory circuit in the hypothalamus. *Nat. Neurosci.* **16**, 1637–1643 (2013).
40. Kawachi, H., Kawazoe, I., Tsubokawa, M., Kishida, M. & Baker, B. I. Characterization of melanin-concentrating hormone in chum salmon pituitaries. *Nature* **305**, 321–323 (1983).

Acknowledgements We thank all members of the Mourrain laboratory for helpful feedback and discussion during the project and preparation of the manuscript; L. de Lecea, J. Zeitzer, C. Heller, D. Grahn, D. Colas and A. Adamantidis for important feedback; P. Raymond, K. Kwan and H. Burgess for sharing constructs and lines; S. Nishino for the kind gift of zolpidem; L. Alexandre and S. Murphy for their diligent care of our zebrafish; Stanford Cell Sciences Imaging Facility for imaging assistance (funded by NCRR award S10RR02557401); and J. Goldberg (Research To Prevent Blindness) and Stanford Vision Research Core (NIH P30-EY0268771). Funding support was provided by Stanford School of Medicine Dean’s fellowship (L.C.L.); JP18H04988, NBRP from AMED (K.K.); NIMH, NIDA, DARPA, NSF, Wieggers Family Fund, AE Foundation, Tarlton Foundation, and Gatsby Foundation (K.D.); NIMH, NINDS, Tashia and John Morgridge Fund (A.E.U.); and NIDDK (5R01DK090065-05), NINDS, NIMH, NIA, Bright-Focus Foundation, Simons Foundation and John Merck Fund (P.M.).

Reviewer information Nature thanks Herwig Baier and the other anonymous reviewer(s) for their contribution to the peer review of this work.

Author contributions L.C.L., G.X.W. and P.M. conceived the study. L.C.L. and P.M. designed experiments. L.C.L. and G.X.W. built the imaging platform and computing hardware. L.C.L., R.M., K.K. and G.S. performed cloning and generated transgenic lines and mutants. L.C.L. performed all experiments except for two-photon imaging (G.X.W.). L.C.L. and G.X.W. developed and wrote the computational pipeline. L.C.L. performed analysis and produced the figures. K.D. provided project mentorship. A.E.U. provided genome analysis and mentorship. L.C.L. and P.M. wrote the paper with contributions from all authors.

Competing interests The authors declare no competing interests.

Additional information

Extended data is available for this paper at <https://doi.org/10.1038/s41586-019-1336-7>.

Supplementary information is available for this paper at <https://doi.org/10.1038/s41586-019-1336-7>.

Reprints and permissions information is available at <http://www.nature.com/reprints>.

Correspondence and requests for materials should be addressed to P.M.

Publisher’s note: Springer Nature remains neutral with regard to jurisdictional claims in published maps and institutional affiliations.

© The Author(s), under exclusive licence to Springer Nature Limited 2019